

Time evolution of the equation of state during perturbative reheating and its impact on the inflationary tensor perturbation spectrum

Avirup Ghosh^a and Deep Ghosh^b

^a*ARC Centre of Excellence for Dark Matter Particle Physics, School of Physics, The University of Melbourne, Victoria 3010, Australia*

^b*Department of Physical Sciences, Indian Institute of Science Education and Research, Kolkata, Mohanpur - 741246, India*

E-mail: avirup.ghosh1993@gmail.com, matrideb1@gmail.com

ABSTRACT: The spectrum of inflationary tensor perturbations is one of the very few available probes of the post-inflationary reheating epoch, and it is strongly influenced by the Universe's equation of state during this period. In the current era of precision cosmology, an accurate estimation of this primordial tensor perturbation spectrum is crucial. Unlike the conventional assumption of a constant equation of state during the perturbative reheating phase, in this work we dynamically calculate the time evolution of the reheating equation of state for different values of the inflaton decay rates including their possible time-dependence in some cases. We further investigate its impact on the spectrum of primordial tensor perturbations, focusing on two different inflationary potentials of the E-model α -attractor class, with $n = 1$ and $n = 3$. Using this approach, our results indicate that the inflationary tensor perturbations can be enhanced (or suppressed) by a factor of ~ 1.5 – 3 compared to standard calculations assuming a constant inflaton equation of state. Such a variation arises because the evolution of the comoving horizon differs in the two approaches, causing different comoving momentum modes to re-enter the horizon at different times and undergo distinct evolutions.

Contents

1	Introduction	1
2	Dynamics of inflation and post-inflationary reheating	2
3	Propagation of tensor perturbations during reheating era	7
4	Summary and conclusion	11
A	Effect of Primordial Tensor Perturbations on GW evolutions	11

1 Introduction

The early Universe underwent a phase of exponential expansion known as inflation, which is crucial for explaining its large-scale homogeneity and isotropy observed today. However, inflation must have eventually ended, transitioning the Universe into the radiation-dominated era so that the predictions of Big-Bang Nucleosynthesis (BBN) can be correctly reproduced. This transitional phase between the end of inflation and the radiation-dominated era is called the reheating era, during which the energy stored in the inflaton field was transferred presumably into the Standard Model (SM) particles, creating a hot radiation bath. Despite its importance, the reheating era remains one of the least understood epochs in the history of the early Universe due to the lack of direct observational evidence. However, this phase may have been the stage for several interesting phenomena, such as, the dark matter production, matter-antimatter asymmetry generation [1–4] and hence, understanding the physics of reheating is essential to gain deeper insights into the evolution of the early Universe.

Inflation not only explains the large-scale homogeneity and isotropy of the present-day Universe but also provides a natural mechanism for the origin of primordial perturbations [5–8]. The scalar component of these perturbations, arising from quantum fluctuations during inflation, serve as the seeds for the formation of large-scale structures like galaxies and clusters. Moreover, inflation predicts the existence of tensor perturbations, as well, which manifest as inflationary gravitational waves (GWs). Detecting these GWs would offer strong evidence in favour of the theory of slow-roll inflation. Recent advancements in gravitational wave astronomy, such as the GW detections by LIGO [9], NANOGrav [10], and other observatories, have spurred new proposals to detect GWs across a wide range of frequencies [11–16]. Such efforts could significantly enhance our understanding of the inflationary dynamics and provide deeper insights into the early Universe.

The inflationary tensor perturbations exit the cosmological horizon due to the rapid decrease in the size of the comoving horizon during inflation and later, as the Universe further evolves the comoving horizon gradually increases and these perturbations reenter the horizon. After this, such comoving modes pass through various phases, including reheating, radiation-domination, matter-domination etc. Since the gravitational waves interact very weakly with matter and radiation, they travel almost unaffected from their origin till the present day. This makes them a remarkably clean probe for studying the physics of the early Universe. In particular, the primordial GW spectrum encodes information about the inflationary era and the subsequent reheating phase. Thus, by observing the primordial GW spectrum, one can reveal the details about the reheating epoch. This potential has motivated extensive studies, as the next-generation of gravitational wave detectors

provide a unique opportunity to test and refine our understanding of the physics of the early Universe (see, for example, [17, 18, 20, 21, 34]).

Specifically, the equation of state (EOS) of the Universe ($w = p_{\text{tot}}/\rho_{\text{tot}}$) during the reheating era plays a crucial role in shaping the primordial tensor perturbations spectra. With the advancements in the next-generation of gravitational wave (GW) detectors, there exists an increasing opportunity to accurately probe these spectra, which could enhance our understanding of the physics at play during reheating [17, 18, 20, 21, 34]. However, most of the earlier studies in this direction have considered the inflaton EOS w_ϕ to be a constant during reheating, but such an approximation is not always true. For example, in refs. [22–25] it has been shown that the time-varying inflaton EOS can stem from an era of non-perturbative particle production following the inflation. In particular, the authors of ref. [25] have parametrized the inflaton EOS, taking inputs from lattice simulations performed for specific models involving inflaton and other fields. *On the contrary, in the present work we show the evolution of the inflation EOS within the perturbative reheating epoch for specific inflationary potentials, while being agnostic about the underlying model that dictates the inflaton decay rates to the visible sector.* Consequently, we demonstrate its imminent impact on the inflationary tensor perturbations for different cosmological histories stemming from different inflaton decay rates.

With these motivations, we have considered two different inflationary potentials of the E-model α -attractor class and fixed all relevant parameters using the Cosmic Microwave Background (CMB) data of the scalar-spectral index n_s and the amplitude of the scalar perturbations A_s . Following which, we have solved the evolution equations of the inflaton energy density and radiation energy density during the reheating era to determine the time-evolution of the reheating EOS w_{RH} dynamically for different values of the inflaton decay rates, including their possible time dependence in some cases. This allows us to track the evolution of the comoving hubble radius ($1/aH$) during reheating era which impacts the spectra of primordial tensor perturbations reentering the comoving horizon during the reheating epoch. Finally, we find that our approach of using the time-varying w_{RH} predicts a present-day GW spectrum which is enhanced (or suppressed) compared to that predicted assuming a constant inflaton-EOS, by a factor of $\sim 1.5 - 3$. Although such an $\mathcal{O}(1)$ improvement can be very hard to decipher in the next-generation of gravitational wave observations due to various systematic uncertainties, we still think it is crucial to point out such effects, as we gradually move towards an era of increasingly precise gravitational wave astronomy.

This paper is organized as follows: In Sec. 2, we have obtained the evolutions of the reheating EOS and also the evolutions of the comoving horizon of the Universe during the perturbative reheating era. Sec. 3 is devoted to determine the evolution of the tensor perturbations during reheating epoch and to obtain the impact of the time-variation of w_ϕ on the present-day GW spectrum. In Sec. 4, we summarize and conclude, while in Appendix.A, we show the slight scale variance of primordial tensor power spectrum for large wavelengths.

2 Dynamics of inflation and post-inflationary reheating

Given a single-field potential $V(\phi)$, the inflationary dynamics is determined by the following slow-roll parameters:

$$\epsilon(k_*) = \frac{M_{\text{Pl}}^2}{2} \left(\frac{V'(\phi)}{V(\phi)} \right)^2 \Big|_{\phi=\phi_*}, \quad \eta(k_*) = M_{\text{Pl}}^2 \left(\frac{V''(\phi)}{V(\phi)} \right) \Big|_{\phi=\phi_*}, \quad (2.1)$$

where $'$ denotes derivative w.r.t ϕ , k_* is the CMB pivot scale 0.05 Mpc^{-1} and ϕ_* is the value of ϕ when k_* exits the horizon. These slow-roll parameters are directly related to the CMB observables, i.e., the scalar tilt n_s , amplitude of density perturbations A_s and the tensor-to-scalar ratio r , as

follows:

$$n_s = 1 + 2\eta - 6\epsilon, A_s = \frac{1}{24\pi^2\epsilon} \frac{V(\phi)}{M_{\text{Pl}}^4}, r = 16\epsilon. \quad (2.2)$$

The recent Planck data [26] suggests $n_s = 0.9649 \pm 0.0044$, $A_s = (2.105 \pm 0.029) \times 10^{-9}$ and $r < 0.1$ at the pivot momentum $k_* = 0.05 \text{ Mpc}^{-1}$, which can be utilised to constrain the parameters of any given inflationary model.

While most of the monomial models of chaotic inflation fail to comply with the recent Planck data, the α -attractor models are one class of models that fit the current CMB data (see [27]) quite well. Apart from their consistency with the CMB data these models are also motivated from several theoretical perspectives. Most of these α -attractor models can actually arise from supergravity and can also explain supersymmetry breaking [28]. Additionally, the possible origin of the late time cosmological constant driven expansion can also be obtained within such models [29]. Hence, in this work, we have considered the general class of the E-model α -attractor potential:

$$V(\phi) = \lambda M_{\text{Pl}}^4 \left(1 - e^{-\sqrt{2/3}\alpha\phi/M_{\text{Pl}}}\right)^{2n} \simeq \left(\frac{2}{3\alpha}\right)^n \lambda M_{\text{Pl}}^4 (\phi/M_{\text{Pl}})^{2n}, \text{ about } \phi = 0 \quad (2.3)$$

for which,

$$n_s = \frac{1 - 2\left(1 + \frac{4n}{3\alpha}\right)e^{-\sqrt{2/3}\alpha\phi/M_{\text{Pl}}} + \left(1 - \frac{8n^2}{3\alpha}\right)e^{-2\sqrt{2/3}\alpha\phi/M_{\text{Pl}}}}{\left(1 - e^{-\sqrt{2/3}\alpha\phi/M_{\text{Pl}}}\right)^2}, \quad (2.4)$$

$$A_s = \frac{\alpha\lambda}{32n^2\pi^2} e^{2\sqrt{2/3}\alpha\phi/M_{\text{Pl}}} \left(1 - e^{-\sqrt{2/3}\alpha\phi/M_{\text{Pl}}}\right)^{2(1+n)}, \quad (2.5)$$

$$r = \frac{64n^2}{3\alpha} \frac{e^{-2\sqrt{2/3}\alpha\phi/M_{\text{Pl}}}}{\left(1 - e^{-\sqrt{2/3}\alpha\phi/M_{\text{Pl}}}\right)^2}, \quad (2.6)$$

$$N_k = \frac{1}{M_{\text{Pl}}^2} \int_{\phi_{\text{end}}}^{\phi_k} d\phi \frac{V(\phi)}{V'(\phi)} = \frac{1}{M_{\text{Pl}}^2} \int_{\phi_{\text{end}}}^{\phi_k} d\phi \sqrt{\frac{3\alpha}{2}} \frac{\left(e^{\sqrt{2/3}\alpha\phi/M_{\text{Pl}}} - 1\right)}{2n/M_{\text{Pl}}}. \quad (2.7)$$

N_k is number of e -foldings until the horizon exit of the pivot scale during the inflation. Assuming $\alpha = 1$ and using the central values of n_s , A_s and $\epsilon(\phi_{\text{end}}) = r(\phi_{\text{end}})/16 = 1$ (inflation ends at $\phi = \phi_{\text{end}}$), we obtain the parameters for two different potentials with $n = 1$ and $n = 3$, which are shown in tab. 1. At the end of inflation, $\epsilon(\phi_{\text{end}}) \simeq \frac{3}{2} \dot{\phi}^2 / \rho_{\phi}|_{\phi_{\text{end}}} \sim 1$, $\dot{\phi} \sim \sqrt{V(\phi_{\text{end}})}$ and hence, $\rho_{\phi} \sim 3V(\phi_{\text{end}})/2 \equiv \rho_{\text{end}}$. We also assume the energy density in radiation, i.e., ρ_R , to be 0 at the end of inflation. N_k is calculated with the knowledge of ϕ_k and ϕ_{end} . In the slow roll approximation, ϕ_{end} becomes known and ϕ_k is derived using measurement of n_s in the CMB scale. In particular, for quadratic inflaton potential, $N_k \approx (3 + n_s)/2(1 - n_s)$.

For $\phi < \phi_{\text{end}}$, the inflaton field ϕ starts oscillating about the minimum of $V(\phi)$, following the eq:

$$\ddot{\phi} + (3H + \Gamma)\dot{\phi} + V'(\phi) = 0, \quad (2.8)$$

where H is the hubble rate, $V'(\phi) = dV(\phi)/d\phi$ and Γ represents the decay rate of the inflaton condensate. The decay rate can be either time-independent or time-dependent, depending on the inflaton potential during the reheating phase. For example, for quadratic potential, the inflaton mass becomes time-independent thereby the decay rate can be parametrized by a time-independent quantity, while for the sextic potential it becomes time-dependent, stemming from the time-varying oscillation amplitude of the inflaton condensate. For details see Refs.[30, 31]. In this study we have shown the effect of time-dependent decay rate of the inflaton on the EOS of the reheating phase (see Fig.2), subsequently on the tensor power spectrum (see the right panel of Fig.5) for the α -attractor model with $n = 3$.

Model	λ	ϕ_*/M_{Pl}	$\phi_{\text{end}}/M_{\text{Pl}}$	r	N_k	a_{end}
E-model ($\alpha = 1, n = 1$) $\lambda M_{\text{Pl}}^4 \left(1 - e^{-\sqrt{2/3}\phi/M_{\text{Pl}}}\right)^2$ $\simeq \frac{14}{23} \lambda M_{\text{Pl}}^4 (\phi/M_{\text{Pl}})^2$	1.12×10^{-10}	5.35	0.94	0.003	55	1.47×10^{-29}
E-model ($\alpha = 1, n = 3$) $\lambda M_{\text{Pl}}^4 \left(1 - e^{-\sqrt{2/3}\phi/M_{\text{Pl}}}\right)^6$ $\simeq \frac{8}{27} \lambda M_{\text{Pl}}^4 (\phi/M_{\text{Pl}})^6$	1.14×10^{-10}	6.67	1.83	0.003	56	5.03×10^{-29}

Table 1: Constraints imposed by the Planck CMB data ($n_s = 0.9649$, $A_s = 2.105 \times 10^{-9}$ at the pivot scale $k_* = 0.05 \text{ Mpc}^{-1}$) [26] on the parameters of the chosen inflationary potentials are presented. The inflation field starts oscillation from $\phi = \phi_{\text{end}}$. N_k is the number of e -foldings until the horizon exit of the pivot scale during the inflation.

Moreover, as mentioned in the introduction, our study points out the effect of the shape of the inflaton potential on the inflaton EOS during the perturbative reheating epoch and hence the possibility of an era of non-perturbative particle production following inflation has been ignored here. For the effect of the non-perturbative particle production on inflaton EOS we refer the reader to [25].

The energy density and the pressure density of the field ϕ are given by,

$$\rho_\phi = \frac{\dot{\phi}^2}{2} + V(\phi), \quad (2.9)$$

$$p_\phi = \frac{\dot{\phi}^2}{2} - V(\phi), \quad (2.10)$$

and combining eqs.2.9 and 2.10 with eq. 2.8 we obtain,

$$\frac{d\rho_\phi}{dt} + 3H(1+w_\phi)\rho_\phi = -\Gamma(1+w_\phi)\rho_\phi, \quad (2.11)$$

which dictates the evolution of the inflaton energy density during the reheating era. On the other hand, from the conservation of the energy-momentum tensor we get:

$$\frac{d\rho_{\text{tot}}}{dt} + 3H(1+w_{\text{RH}})\rho_{\text{tot}} = 0, \quad (2.12)$$

from which one obtains the evolution of the radiation energy density as follows,

$$\frac{d\rho_R}{dt} + 4H\rho_R = \Gamma(1+w_\phi)\rho_\phi, \quad (2.13)$$

where the inflaton equation of state (EOS) $w_\phi = p_\phi/\rho_\phi$ and the reheating EOS w_{RH} is given by:

$$w_{\text{RH}} = \frac{w_\phi\rho_\phi + \rho_R/3}{\rho_\phi + \rho_R}, \quad (2.14)$$

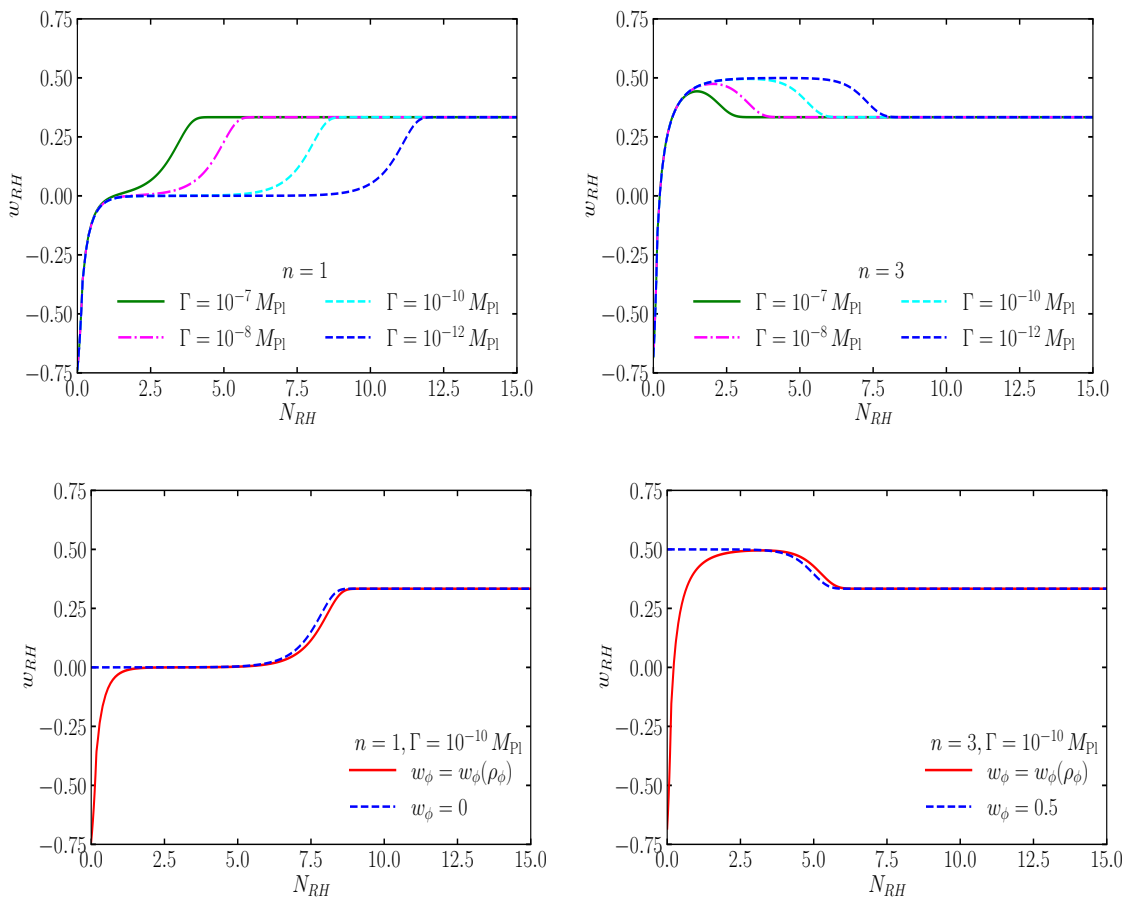


Figure 1: *Top:* Evolution of the reheating EOS w_{RH} during reheating era is shown as a function of the reheating e -foldings N_{RH} for the E-model α -attractor potential with $n = 1$ (left) and $n = 3$ (right). Here the four different values of the inflaton decay rate Γ have been considered. *Bottom:* Assuming $\Gamma = 10^{-10} M_{\text{Pl}}$, we have shown the evolutions of w_{RH} for constant inflaton-EOS (blue dashed) and exact EOS (red solid) for E-model α -attractor potential with $n = 1$ (left) and $n = 3$ (right). See the text for details.

assuming the Universe to be a two-fluid system during the reheating era.

Therefore, eqs. 2.11 and 2.13 together imply that the dynamics of reheating is affected by the value of w_ϕ and following [32], w_ϕ can be written as,

$$w_\phi(\rho_\phi) = 2 \frac{\int_{\phi_{m1}}^{\phi_{m2}} d\phi \sqrt{1 - V(\phi)/\rho_\phi}}{\int_{\phi_{m1}}^{\phi_{m2}} d\phi / \sqrt{1 - V(\phi)/\rho_\phi}} - 1, \quad (2.15)$$

where $\phi_{m1,m2}$ represent the amplitudes of inflaton oscillations during the reheating era. The formula in eq. 2.15 can capture the variations in w_ϕ even when the inflationary potential $V(\phi)$ is not absolutely symmetric around the minima of the Potential. For our chosen set of potentials, these

are given as follows,

$$\phi_{m1,m2}(\rho_\phi) = \sqrt{\frac{3}{2}} M_{\text{Pl}} \ln \left[\frac{1}{1 \pm \left(\frac{\rho_\phi}{\lambda M_{\text{Pl}}^4} \right)^{1/2n}} \right]. \quad (2.16)$$

Using eq. 2.15 we first obtain the inflaton EOS $w_\phi(\rho_\phi)$ as a function of the inflaton energy density ρ_ϕ and then use it to solve the eqs. 2.11 and 2.13. Hereafter, we call this approach to be ‘actual EOS’ approach. The resulting evolutions of ρ_ϕ and ρ_R are then used to obtain the reheating EOS w_{RH} from eq. 2.14. In the top panel of Fig. 1 we have shown the evolutions of w_{RH} for $n = 1$ (left) and $n = 3$ (right) for several values of the inflaton decay rate Γ .

Note that, if one approximates the potentials by the leading terms of their Taylor-series expansions about their corresponding minima, eq. 2.15 gives $w_\phi = 0$ for $n = 1$ and $w_\phi = 0.5$ for $n = 3$, respectively. We also solve eqs. 2.11 and 2.13 using these constant values of w_ϕ and hereafter refer this approach as the ‘constant inflaton-EOS’ approach. In the bottom panel of Fig. 1 we have compared the evolutions of w_{RH} as obtained in the actual EOS case (red solid) and in the constant inflaton-EOS approach (blue dashed) for $n = 1$ (left) and $n = 3$ (right) assuming $\Gamma = 10^{-10} M_{\text{Pl}}$.

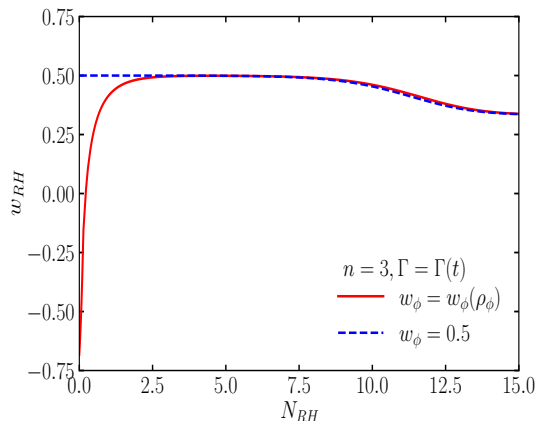


Figure 2: For the $n = 3$ case, we have shown the differences of the evolutions of w_{RH} for constant inflaton-EOS (blue dashed) and exact EOS (red solid) assuming time-dependent inflaton decay rate. See text for details.

In addition, as mentioned earlier we have also considered a case of time-dependent decay rate for the inflaton in $n = 3$ model. Assuming the inflaton decays into fermions dominantly we use [30]:

$$\Gamma(t) = M_{\text{Pl}} \frac{y^2}{8\pi} \sqrt{\left(\frac{2}{3\alpha} \right)^n 2n(2n-1) \lambda \alpha_y \frac{\omega}{m_\phi} \left(\frac{\rho_\phi}{M_{\text{Pl}}^4} \right)^{\frac{n-1}{2n}}}, \quad (2.17)$$

which for $n = 3$ is given by, $\Gamma(t) = 4.61 \times 10^{-7} M_{\text{Pl}} y^2 \left(\frac{\rho_\phi}{M_{\text{Pl}}^4} \right)^{\frac{1}{3}}$ [30] where y represents the Yukawa coupling between the inflaton ϕ and the daughter fermions. Choosing $y = 1$ and putting the resulting $\Gamma = \Gamma(t)$ in eqs. 2.11 and 2.13 we track the evolution of w_{RH} for both constant $w_\phi = 0.5$ and actual w_ϕ (obtained from eq. 2.15), which are presented in Fig. 2.

As will be evident later, another quantity of interest for our study is the comoving horizon ($1/aH$) of the Universe during the reheating era. The inverse of the comoving horizon in the

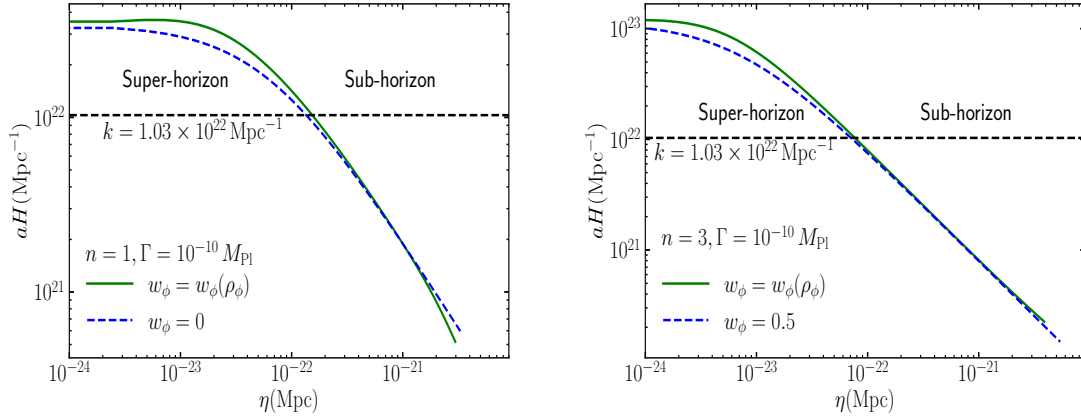


Figure 3: For the E-model α -attractor potential with $n = 1$ (left) and $n = 3$ (right), the evolution of aH have been shown as a function of the comoving time η . In each case, the blue dashed line shows the result obtained assuming a constant inflaton-EOS and the green solid line shows the evolution when the time-varying EOS is considered. Here $\Gamma = 10^{-10} M_{\text{Pl}}$ is assumed. See the text for details.

constant EOS approach is given by,

$$aH(N) = \frac{a_{\text{end}} \sqrt{\rho_{\text{end}}}}{\sqrt{3} M_{\text{Pl}}} e^{-N(1+3w_\phi)/2}. \quad (2.18)$$

On the other hand, this same quantity for the actual EOS approach is obtained as follows,

$$aH(N) = \frac{a_{\text{end}} \sqrt{\rho_{\text{end}}}}{\sqrt{3} M_{\text{Pl}}} e^{N-3 \int_0^N dN' (1+w_{\text{RH}}(N'))}. \quad (2.19)$$

We have defined the end of reheating by the condition $\rho_\phi = \rho_R$. The differences of these quantities are evident from Fig. 3 where we have shown aH as a function of the comoving time $\eta = \int da/a^2 H$ for $n = 1$ (left) and $n = 3$ (right), respectively. In both the cases, we have considered $\Gamma = 10^{-10} M_{\text{Pl}}$ and have represented the results obtained for the constant inflaton-EOS approach by blue dashed lines while that for the actual EOS case by the green solid lines. The black dashed line represents a particular comoving momentum $k = 1.03 \times 10^{22} \text{ Mpc}^{-1}$ which enters the horizon during the reheating era and hence will carry the imprints of the physics occurring during the reheating era.

3 Propagation of tensor perturbations during reheating era

As mentioned earlier, inflationary tensor perturbations (or gravitational waves) can provide new avenues to unveil the dynamics of reheating era thanks to the current advancements in the field of GW astronomy [17, 18, 20, 21, 34]. Therefore, in this section, we seek to investigate how does the reheating eq. of states obtained in the constant EOS approach and in the actual EOS approach affect the inflationary tensor perturbation spectra.

During inflation, the comoving hubble radius ($1/aH$) decreases and any particular comoving momentum mode k of tensor perturbations produced during inflation become super-horizon when $k < aH$. After inflation, the comoving hubble radius ($1/aH$) increases and some of the super-horizon modes which earlier exited, reenter the horizon. After reentering the horizon such modes

experience the effects of the evolution of the Universe and propagate following,

$$\ddot{h}_k + \frac{3\dot{a}}{a}\dot{h}_k + \frac{k^2}{a^2}h_k = 0, \quad (3.1)$$

in absence of any additional source term. In eq. 3.1, h_k represents the fourier transform of the amplitude of mode k and the polarization index is suppressed for brevity. When written in terms of the comoving time η , eq. 3.1 becomes,

$$h_k'' + 2aHh_k' + k^2h_k = 0, \quad (3.2)$$

where $'$ denotes the derivative w.r.t η . Eq. 3.2 can be further rewritten as:

$$\frac{d^2h_k}{d(k\eta)^2} + 2\left(\frac{aH}{k}\right)\frac{dh_k}{d(k\eta)} + h_k = 0, \quad (3.3)$$

which is simply the equation of motion of a damped harmonic oscillator with time-dependent damping term, aH/k . Therefore, for any given comoving momentum $k \ll aH$ eq. 3.3 has the solution $h_k = \text{const}$ and the amplitude of the GW spectrum remains unchanged. On the other hand, for any given comoving momentum $k \gtrsim aH$, the amplitude of GW spectrum damps as the Universe evolves. To obtain the exact evolution of the GW spectra for constant inflaton-EOS and actual EOS approaches we solve eq. 3.3 numerically, using the $aH(\eta)$ obtained in sec. 2.

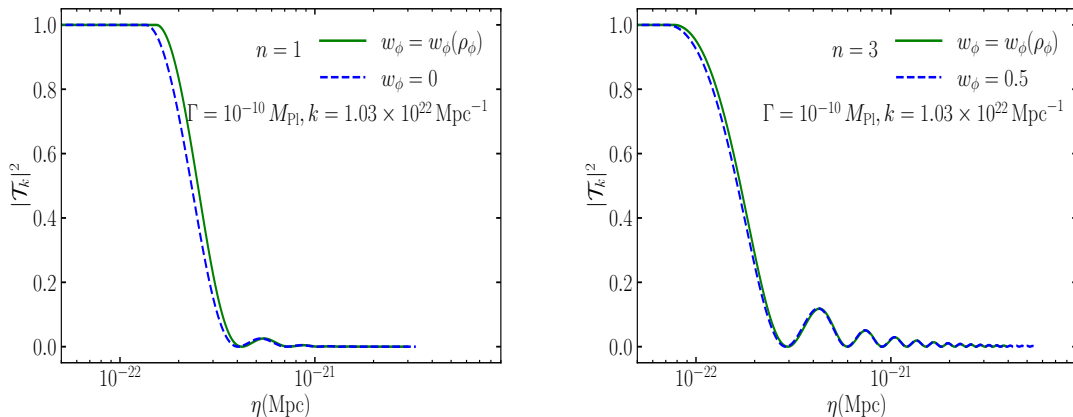


Figure 4: The evolution of a particular comoving momentum mode $k = 1.03 \times 10^{22} \text{ Mpc}^{-1}$ of tensor perturbations, that enters the horizon during reheating, is shown for $n = 1$ (left) and $n = 3$ (right) assuming constant inflaton-EOS (blue dashed line) and actual EOS (green solid line), respectively. Here $\Gamma = 10^{-10} M_{\text{Pl}}$ is assumed. See the text for details.

To this end, we define the transfer function and its derivative as, $\mathcal{T}_k(\eta) = h_k^-(\eta)/h_k^{\text{prim}}$ and $\mathcal{T}_k'(\eta) = h_k'^-(\eta)/h_k^{\text{prim}}$, respectively, with h_k^{prim} representing the amplitude of mode k at the horizon exit during inflation. Evolution of $|\mathcal{T}_k(\eta)|^2$ for the mode $k = 1.03 \times 10^{22} \text{ Mpc}^{-1}$ during perturbative reheating era are shown in Fig. 4 for $n = 1$ (left) and $n = 3$ (right), assuming, $\Gamma = 10^{-10} M_{\text{Pl}}$. Here, the blue dashed lines show the result for constant inflaton-EOS and the green solid lines are obtained considering the actual evolution of w_{RH} . Clearly, the differences between the transfer functions obtained in the two different approaches stem from when a particular comoving momentum mode reenters the horizon and also from the instant of time signifying the end of the reheating era. As we shall see later, these can have substantial impact on the present-day spectrum of inflationary tensor perturbations.

After the end of reheating, the standard radiation domination takes over and the amplitude of tensor perturbations evolve as:

$$h_k^{\text{RD}}(\eta) = \sqrt{\frac{2}{\pi}} [C_1^k j_0(k\eta) + C_2^k y_0(k\eta)] h_k^{\text{prim}}. \quad (3.4)$$

We choose the coefficients $C_{1,2}^k$ such that at $\eta = \eta_{\text{RH}}$ our solutions for $\mathcal{T}_k(\eta_{\text{RH}})$ matches with eq. 3.4:

$$C_1^k = \sqrt{\frac{\pi}{2}} \left(\frac{y_1(k\eta_{\text{RH}})\mathcal{T}_k(\eta_{\text{RH}}) - y_0(k\eta_{\text{RH}})\mathcal{T}'_k(\eta_{\text{RH}})}{j_0(k\eta_{\text{RH}})y_1(k\eta_{\text{RH}}) - y_0(k\eta_{\text{RH}})j_1(k\eta_{\text{RH}})} \right), \quad (3.5)$$

$$C_2^k = -\sqrt{\frac{\pi}{2}} \left(\frac{j_1(k\eta_{\text{RH}})\mathcal{T}_k(\eta_{\text{RH}}) - j_0(k\eta_{\text{RH}})\mathcal{T}'_k(\eta_{\text{RH}})}{j_0(k\eta_{\text{RH}})y_1(k\eta_{\text{RH}}) - y_0(k\eta_{\text{RH}})j_1(k\eta_{\text{RH}})} \right). \quad (3.6)$$

Similarly, at the matter-radiation equality, $\eta = \eta_{\text{eq}}$, it is ensured that the solutions smoothly transit to the solutions in matter-dominated era, given by:

$$h_k^{\text{MD}}(\eta) = \sqrt{\frac{2}{\pi}} \frac{\eta_{\text{eq}}}{\eta} [D_1^k j_1(k\eta) + D_2^k y_1(k\eta)] h_k^{\text{prim}}, \quad (3.7)$$

with

$$D_1^k = \left[C_1^k \left(\frac{3}{2k\eta_{\text{eq}}} - \frac{\cos(2k\eta_{\text{eq}})}{2k\eta_{\text{eq}}} + \frac{\sin(2k\eta_{\text{eq}})}{(k\eta_{\text{eq}})^2} \right) + C_2^k \left(1 - \frac{1}{(k\eta_{\text{eq}})^2} - \frac{\cos(2k\eta_{\text{eq}})}{(k\eta_{\text{eq}})^2} - \frac{\sin(2k\eta_{\text{eq}})}{2k\eta_{\text{eq}}} \right) \right], \quad (3.8)$$

$$D_2^k = \left[C_1^k \left(-1 + \frac{1}{(k\eta_{\text{eq}})^2} - \frac{\cos(2k\eta_{\text{eq}})}{(k\eta_{\text{eq}})^2} - \frac{\sin(2k\eta_{\text{eq}})}{2k\eta_{\text{eq}}} \right) + C_2^k \left(\frac{3}{2k\eta_{\text{eq}}} + \frac{\cos(2k\eta_{\text{eq}})}{2k\eta_{\text{eq}}} - \frac{\sin(2k\eta_{\text{eq}})}{(k\eta_{\text{eq}})^2} \right) \right]. \quad (3.9)$$

Ignoring the small period of dark energy domination in the late Universe, the amplitude of tensor perturbations today (i.e., at $\eta = \eta_0$), is given by,

$$h_k(\eta_0) = \sqrt{\frac{2}{\pi}} \frac{\eta_{\text{eq}}}{\eta_0} [D_1^k j_1(k\eta_0) + D_2^k y_1(k\eta_0)] h_k^{\text{prim}}. \quad (3.10)$$

Now using eq. 3.10 we obtain the GW spectral energy density today,

$$\frac{d\rho_{\text{GW}}}{d \ln k} = \frac{M_{\text{Pl}}^2}{4 a^2(\eta_0)} \sum_{+, \times} \frac{2k^3}{2\pi^2} \langle |h'_k(\eta_0)|^2 \rangle. \quad (3.11)$$

Using eq. 3.10 and introducing the definition of primordial power spectrum $\Delta_{k,\text{inf}}^2 = \sum_{+, \times} \frac{2k^3}{2\pi^2} \langle |h_k^{\text{prim}}|^2 \rangle$ ¹, eq. 3.11 can be re-expressed as,

$$\frac{d\rho_{\text{GW}}}{d \ln k} = \frac{M_{\text{Pl}}^2 k^2}{4 a^2(\eta_0)} \Delta_{k,\text{inf}}^2 \left\langle \left| \frac{dh_k(\eta)/h_k^{\text{prim}}}{d(k\eta)} \right|_{\eta=\eta_0}^2 \right\rangle, \quad (3.12)$$

where $\langle \dots \rangle$ represents average over multiple oscillations. The relative energy density in GW today is,

$$\Omega_{\text{GW}}^0 = \frac{1}{\rho_c} \frac{d\rho_{\text{GW}}}{d \ln k} = \frac{k^2}{12 a^2(\eta_0) H^2(\eta_0)} \Delta_{k,\text{inf}}^2 \left\langle \left| \frac{dh_k(\eta)/h_k^{\text{prim}}}{d(k\eta)} \right|_{\eta=\eta_0}^2 \right\rangle, \quad (3.13)$$

¹Note that, the primordial tensor power-spectrum $\Delta_{k,\text{inf}}^2 \equiv P_T$ is strictly scale-invariant for $k \approx k_*$, but can vary slightly for large- k , as shown in [33, 34]. The effect of such variation is presented in Appendix A.

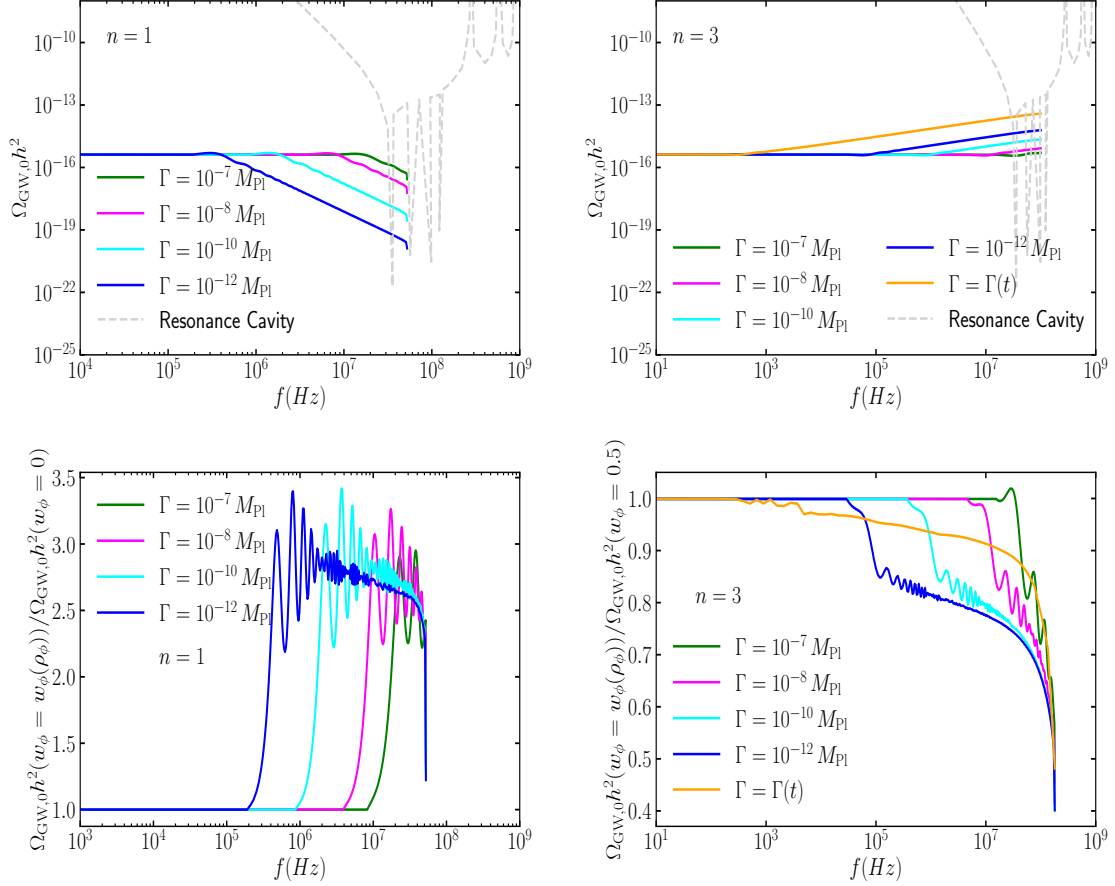


Figure 5: *Top:* The present day spectrum of inflationary gravitational waves (GW) for the E-model α -attractor potential with $n = 1$ (left) and $n = 3$ (right) are shown for different values of inflaton decay rate considering actual EOS. The gray dashed curves show the projected sensitivity of the proposed resonance cavity observations. *Bottom:* The ratio of the GW energy density considering actual EOS to that obtained for constant inflaton-EOS are shown for $n = 1$ (left) and $n = 3$ (right), for different choices of Γ . See the text for details.

where the comoving momentum k has an one-to-one correspondence with the frequency of GW signal $f = k/2\pi a_0$. In our calculation of Ω_{GW}^0 (eq. 3.13) we have used $\eta_{\text{eq}} = a_{\text{eq}}/H_0 \sqrt{\Omega_{R,0}}$, $\eta_0 = \eta_{\text{eq}} \sqrt{\Omega_{M,0}/\Omega_{R,0}}$ and $H_0 = 100h \text{ km s}^{-1} \text{ Mpc}^{-1}$ with $h = 0.68$ [26].

The quantity $\Omega_{\text{GW}}^0 h^2$ for the E-model α -attractor potential with $n = 1$ and $n = 3$ are shown for different values of Γ in the top left and top right panels of Fig. 5, respectively. Clearly, as obtained in the constant inflaton-EOS case, the GW spectrum is red-tilted for $n = 1$ and blue-tilted for $n = 3$. The ratio of $\Omega_{\text{GW}}^0 h^2$ for actual EOS to $\Omega_{\text{GW}}^0 h^2$ for constant inflaton-EOS are presented in the bottom panel of Fig. 5 for several values of Γ . Here, it is clear that for $n = 1$ case (left) the GW spectrum is enhanced by a factor of ~ 3 while for $n = 3$ (right) it is suppressed by a factor of ~ 1.5 . Note that, this enhancement or suppression in the GW spectrum is independent of whether Γ is chosen to be a constant or it has a specified time dependence. This is evident from our choice of $\Gamma = \Gamma(t)$ in the $n = 3$ model the results for which are shown by orange lines in both top-right and bottom-right panels of Fig. 5. The gray dashed curves show the sensitivity of the recently proposed

resonance cavity experiments [35, 36] which may be effective in deciphering the high-frequency tail of the inflationary tensor perturbation spectrum.

4 Summary and conclusion

The early universe transits from an inflationary phase to the radiation-dominated phase through an era of reheating, facilitated by the dissipation of the inflaton field to the SM degrees of freedom. One of the well-known mechanisms is the perturbative decay of the inflaton field during its oscillation. During this perturbative reheating epoch, several physical phenomena might have occurred. However, there are currently very few probes available to unveil the physics occurring during this reheating phase, one of which is the inflationary tensor perturbation spectra. This spectra is highly sensitive to the equation of state (EOS) of the Universe during reheating. Given the upcoming era of gravitational wave (GW) astronomy, it is crucial to understand how the EOS of the Universe during the reheating era is influenced by the dynamics occurring at that time and how this, in turn, impacts the spectrum of inflationary tensor perturbations.

In this study, we highlighted that the shape of the inflationary potential during perturbative reheating era can affect the EOS of the Universe, thereby also influencing the spectrum of inflationary tensor perturbations. We have considered two different classes of the E-model α -attractor inflationary potentials with $n = 1$ and $n = 3$ and studied the dynamics of the post-inflationary reheating era using two distinct approaches. In the first approach, the inflaton EOS is assumed to be a constant, while in the second approach, we account for the proper time evolution of the inflaton EOS. Beside determining the time evolution of the reheating EOS for various values of the inflaton decay rates, we also calculated how the propagation of primordial tensor perturbations is affected by this evolution of the reheating EOS. Our findings indicate that the inflationary tensor perturbations can be enhanced or suppressed by a factor of approximately 1.5-3, depending on the specifics of the inflationary potential and the inflaton decay rate assumed. Notably, for both the models, the present-day gravitational wave spectrum is expected to lie within the sensitivity range of the proposed resonance cavity experiments, making them likely to be measured with considerable accuracy.

A Effect of Primordial Tensor Perturbations on GW evolutions

It is clear from eq. 3.13 that the present-day GW spectrum is sensitive to the exact form of the inflationary tensor perturbation spectrum $\Delta_{k,\text{inf}}^2 (\equiv P_T)$ which is nearly scale-invariant around the pivot scale k_* and is given by, $\Delta_{k,\text{inf}}^2 (\equiv P_T) \simeq 2H_{\text{inf}}^2/\pi^2 M_{\text{pl}}^2$. However, for high-scale reheating scenarios like ours, the comoving modes re-entering the horizon during reheating era corresponds to $k \gg k_*$, at which scale $P_T(k)$ is not strictly scale-invariant and a numerical estimation of $P_T(k)$ is necessary, as pointed out in [33, 34]. In order to quantify the possible impact of this non scale-invariant $P_T(k)$ on our analysis, we numerically solve the tensor perturbation eq. 3.1 during inflation and use the resulting $P_T(k)$ for evaluating the present-day GW spectrum Ω_{GW}^0 following eq. 3.13.

In the left panel of Fig. 6 we compare the analytical power-spectrum with the numerically obtained power-spectrum for wide range of k values in case of $n = 3$ E-model α -attractor potential, which shows that P_T can be suppressed by a factor of ~ 2 for large values of k . In the left panel of Fig. 6 vertical black dotted line represents k_{end} which is the largest comoving mode exiting the horizon during inflation. Using this numerically obtained P_T we also obtain the present-day GW spectrum considering the time-dependent decay rate of the inflaton using actual EOS of the inflaton which is shown in the right panel of Fig. 6 by blue dashed-dotted line. Clearly, the GW spectrum is slightly suppressed at larger frequencies, compared to that obtained with analytic form of P_T (shown by the orange line). However, such a suppression is also obtained if one considers the

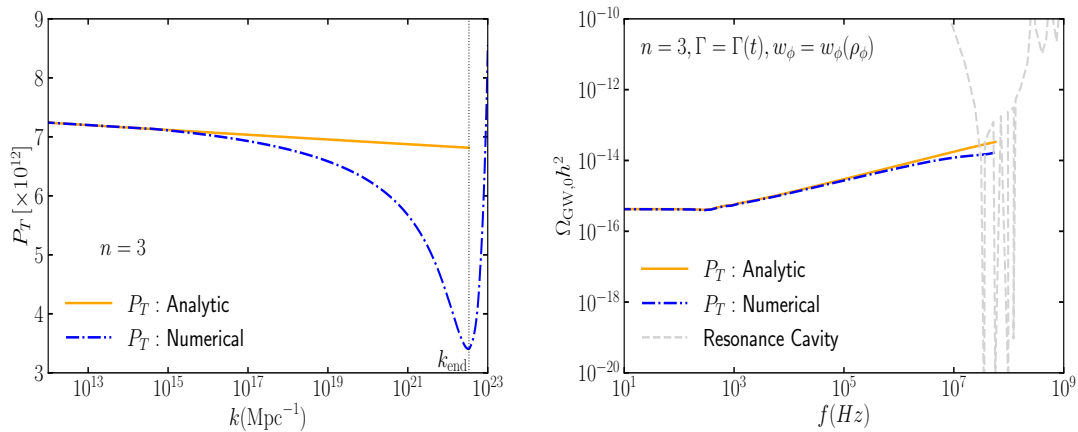


Figure 6: *Left:* In case of $n = 3$, a comparison of analytical vs numerical primordial tensor perturbation spectra (P_T) are shown. *Right:* Assuming time-dependent decay rate and actual inflaton EOS, the resulting present-day GW spectra are shown for $n = 3$ case. See the text for details.

constant inflaton-EOS, and thus the impact of inflaton EOS on the present-day GW spectrum as presented in the main text remains unchanged.

Acknowledgment

A.G. is funded by the ARC Centre of Excellence for Dark Matter Particle Physics, CE200100008. AG and DG thank Satyanarayan Mukhopadhyay for collaborating during the initial stage of the project.

References

- [1] K. Harigaya, M. Kawasaki, K. Mukaida, and M. Yamada, *Dark Matter Production in Late Time Reheating*, *Phys. Rev. D* **89** (2014), no. 8 083532, [[arXiv:1402.2846](#)].
- [2] Y. Mambrini and K. A. Olive, *Gravitational Production of Dark Matter during Reheating*, *Phys. Rev. D* **103** (2021), no. 11 115009, [[arXiv:2102.06214](#)].
- [3] D. S. Gorbunov and A. G. Panin, *Scalaron the mighty: producing dark matter and baryon asymmetry at reheating*, *Phys. Lett. B* **700** (2011) 157–162, [[arXiv:1009.2448](#)].
- [4] A. Dolgov, K. Freese, R. Rangarajan, and M. Srednicki, *Baryogenesis during reheating in natural inflation and comments on spontaneous baryogenesis*, *Phys. Rev. D* **56** (1997) 6155–6165, [[hep-ph/9610405](#)].
- [5] S. W. Hawking, *The Development of Irregularities in a Single Bubble Inflationary Universe*, *Phys. Lett. B* **115** (1982) 295.
- [6] A. H. Guth and S. Y. Pi, *Fluctuations in the New Inflationary Universe*, *Phys. Rev. Lett.* **49** (1982) 1110–1113.
- [7] A. A. Starobinsky, *Dynamics of Phase Transition in the New Inflationary Universe Scenario and Generation of Perturbations*, *Phys. Lett. B* **117** (1982) 175–178.

- [8] J. M. Bardeen, P. J. Steinhardt, and M. S. Turner, *Spontaneous Creation of Almost Scale - Free Density Perturbations in an Inflationary Universe*, *Phys. Rev. D* **28** (1983) 679.
- [9] **LIGO Scientific, Virgo** Collaboration, B. P. Abbott et al., *GW150914: The Advanced LIGO Detectors in the Era of First Discoveries*, *Phys. Rev. Lett.* **116** (2016), no. 13 131103, [[arXiv:1602.03838](#)].
- [10] **NANOGrav** Collaboration, N. S. Pol et al., *Astrophysics Milestones for Pulsar Timing Array Gravitational-wave Detection*, *Astrophys. J. Lett.* **911** (2021), no. 2 L34, [[arXiv:2010.11950](#)].
- [11] **KAGRA, Virgo, LIGO Scientific** Collaboration, R. Abbott et al., *Upper limits on the isotropic gravitational-wave background from Advanced LIGO and Advanced Virgo’s third observing run*, *Phys. Rev. D* **104** (2021), no. 2 022004, [[arXiv:2101.12130](#)].
- [12] M. Branchesi et al., *Science with the Einstein Telescope: a comparison of different designs*, *JCAP* **07** (2023) 068, [[arXiv:2303.15923](#)].
- [13] J. Crowder and N. J. Cornish, *Beyond LISA: Exploring future gravitational wave missions*, *Phys. Rev. D* **72** (2005) 083005, [[gr-qc/0506015](#)].
- [14] N. Seto, S. Kawamura, and T. Nakamura, *Possibility of direct measurement of the acceleration of the universe using 0.1-Hz band laser interferometer gravitational wave antenna in space*, *Phys. Rev. Lett.* **87** (2001) 221103, [[astro-ph/0108011](#)].
- [15] P. Amaro-Seoane et al., *Low-frequency gravitational-wave science with eLISA/NGO*, *Class. Quant. Grav.* **29** (2012) 124016, [[arXiv:1202.0839](#)].
- [16] Low-frequency gravitational-wave science with eLISA/NGOG. Janssen et al., *Gravitational wave astronomy with the SKA, PoS AASKA14* (2015) 037, [[arXiv:1501.00127](#)].
- [17] S. Kuroyanagi, T. Chiba, and N. Sugiyama, *Precision calculations of the gravitational wave background spectrum from inflation*, *Phys. Rev. D* **79** (2009) 103501, [[arXiv:0804.3249](#)].
- [18] D. G. Figueroa and E. H. Tanin, *Ability of LIGO and LISA to probe the equation of state of the early Universe*, *JCAP* **08** (2019) 011, [[arXiv:1905.11960](#)].
- [19] M. R. Haque, D. Maity, T. Paul, and L. Sriramkumar, *Decoding the phases of early and late time reheating through imprints on primordial gravitational waves*, *Phys. Rev. D* **104** (2021), no. 6 063513, [[arXiv:2105.09242](#)].
- [20] S. S. Mishra, V. Sahni, and A. A. Starobinsky, *Curing inflationary degeneracies using reheating predictions and relic gravitational waves*, *JCAP* **05** (2021) 075, [[arXiv:2101.00271](#)].
- [21] A. K. Soman, S. S. Mishra, M. Shafi, and S. Basak, *Inflationary Gravitational Waves as a probe of the unknown post-inflationary primordial Universe*, [arXiv:2407.07956](#).
- [22] S. Antusch, D. G. Figueroa, K. Marschall and F. Torrenti, “Energy distribution and equation of state of the early Universe: matching the end of inflation and the onset of radiation domination,” *Phys. Lett. B* **811**, 135888 (2020) doi:10.1016/j.physletb.2020.135888 [[arXiv:2005.07563](#) [[astro-ph.CO](#)]].
- [23] S. Antusch, D. G. Figueroa, K. Marschall and F. Torrenti, “Characterizing the postinflationary reheating history: Single daughter field with quadratic-quadratic interaction,” *Phys. Rev. D* **105**, no.4, 043532 (2022) doi:10.1103/PhysRevD.105.043532 [[arXiv:2112.11280](#) [[astro-ph.CO](#)]].
- [24] S. Antusch, K. Marschall and F. Torrenti, “Characterizing the post-inflationary reheating history. Part II. Multiple interacting daughter fields,” *JCAP* **02**, 019 (2023) doi:10.1088/1475-7516/2023/02/019 [[arXiv:2206.06319](#) [[astro-ph.CO](#)]].
- [25] P. Saha, S. Anand, and L. Sriramkumar, *Accounting for the time evolution of the equation of state parameter during reheating*, *Phys. Rev. D* **102** (2020), no. 10 103511, [[arXiv:2005.01874](#)].
- [26] **Planck** Collaboration, N. Aghanim et al., *Planck 2018 results. VI. Cosmological parameters*, *Astron. Astrophys.* **641** (2020) A6, [[arXiv:1807.06209](#)]. [Erratum: *Astron. Astrophys.* 652, C4 (2021)].

- [27] **Planck** Collaboration, Y. Akrami et al., *Planck 2018 results. X. Constraints on inflation*, *Astron. Astrophys.* **641** (2020) A10, [[arXiv:1807.06211](#)].
- [28] R. Kallosh and A. Linde, *Planck, LHC, and α -attractors*, *Phys. Rev. D* **91** (2015) 083528, [[arXiv:1502.07733](#)].
- [29] E. V. Linder, *Dark Energy from α -Attractors*, *Phys. Rev. D* **91** (2015), no. 12 123012, [[arXiv:1505.00815](#)].
- [30] M. A. G. Garcia, K. Kaneta, Y. Mambrini, and K. A. Olive, *Inflaton Oscillations and Post-Inflationary Reheating*, *JCAP* **04** (2021) 012, [[arXiv:2012.10756](#)].
- [31] S. Nurmi, T. Tenkanen, and K. Tuominen, *Inflationary Imprints on Dark Matter*, *JCAP* **11** (2015) 001, [[arXiv:1506.04048](#)].
- [32] M. S. Turner, *Coherent Scalar Field Oscillations in an Expanding Universe*, *Phys. Rev. D* **28** (1983) 1243.
- [33] M. A. G. Garcia and A. Pereyra-Flores, *Impact of dark sector preheating on CMB observables*, *JCAP* **08** (2024), 043. [[arXiv:2403.04848](#)]
- [34] M. R. Haque, D. Maity, T. Paul and L. Sriramkumar, *Decoding the phases of early and late time reheating through imprints on primordial gravitational waves*, *Phys. Rev. D* **104** (2021) no.6, 063513 [[arXiv:2105.09242](#)]
- [35] N. Herman, A. Füzfa, L. Lehoucq, and S. Clesse, *Detecting planetary-mass primordial black holes with resonant electromagnetic gravitational-wave detectors*, *Phys. Rev. D* **104** (2021), no. 2 023524, [[arXiv:2012.12189](#)].
- [36] N. Herman, L. Lehoucq, and A. Füzfa, *Electromagnetic antennas for the resonant detection of the stochastic gravitational wave background*, *Phys. Rev. D* **108** (2023), no. 12 124009, [[arXiv:2203.15668](#)].